



Published in final edited form as:

Arterioscler Thromb Vasc Biol. 2014 October ; 34(10): 2217–2223. doi:10.1161/ATVBAHA.114.303036.

Imaging Body Fat: Techniques and Cardiometabolic Implications

H. Wang, Y. E Chen, and D.T. Eitzman

University of Michigan, Department of Internal Medicine, Cardiovascular Research Center, Ann Arbor, Michigan, USA

Abstract

Obesity is a world-wide epidemic and is associated with multiple comorbidities. The mechanisms underlying the relationship between obesity and adverse health outcomes remain poorly understood. This may be due to several factors including the crude measures used to estimate adiposity, the striking heterogeneity between adipose tissue depots, and the influence of fat accumulation in multiple organs. In order to advance our understanding of fat stores and associated co-morbidities in humans, it will be necessary to image adiposity throughout the body and ultimately also assess its functionality. Large clinical studies are demonstrating the prognostic importance of adipose tissue imaging. Newer techniques capable of imaging fat metabolism and other functions of adipose tissue may provide additional prognostic utility and may be useful in guiding therapeutic interventions.

Keywords

obesity; fat composition; adipose tissue imaging

Introduction

Obesity has only relatively recently been acknowledged as a chronic disease.¹ The capacity to readily accumulate fat began as an evolutionary adaptive trait, however, this has become a liability in many countries with wide availability of food supplies and more sedentary lifestyles. The prevalence of obesity has increased over the past several decades to the point where the World Health Organization has declared the global obesity epidemic a worldwide public health crisis.²

The morbidity and mortality associated with obesity is now well documented, however it is also apparent that there is great heterogeneity regarding the health risks associated with obesity. This critical concept has underscored the need for more accurate phenotyping of adipose depots among individuals to determine health risks. Although phenotyping adiposity may eventually be aided with a panel of circulating biomarkers, measurement and imaging of adiposity have been the most predictive of morbidities thus far. To maximize the potential

Corresponding author: Daniel T. Eitzman, MD University of Michigan Cardiovascular Research Center 7301A MSRB III, 1150 West Medical Center Drive Ann Arbor, MI 48109-0644, USA Tel: +1-734-647-9865 Fax: +1-734-936-2641 deitzman@umich.edu.

Disclosure:
None.

of adipose tissue imaging, there is a need for even further refinement of adipose tissue imaging techniques.

The purpose of this review is to provide a brief overview of methods used to measure and image body fat. Other reviews in this miniseries will address differences in adipose depots and health implications in detail.^{3,4}

Measurements of weight and adiposity

Insurance companies were among the first to document the risks associated with obesity. When platform scales became widely available in the second half of the nineteenth century, body weight data became accessible to insurance companies. Louis Dublin (1882-1969), a statistician and vice president of the Metropolitan Life Insurance Company, led studies demonstrating associations between weight, comorbidities, and mortality.⁵ Based on this data, ideal body weights for age and height were reported. To more clearly represent the interdependence of weight and height, astronomer and mathematician Alphonse Quetelet developed the Quetelet Index or body mass index (BMI) (weight (kg)/height (m²)).⁶ This index is still widely used to classify subjects as overweight (BMI > 25) or obese (BMI > 30).

However, BMI is not always a measure of fatness and individuals with high muscle mass may be incorrectly classified as obese - defined as excess body fat that has accumulated to the extent that it may have a negative effect on health, leading to reduced life expectancy and /or increased health problems.⁷

Waist circumference and the waist-to-hip ratio are other measures that may correlate better with body fatness and be more predictive of adverse metabolic effects due to obesity, as well as cardiovascular complications. For example, in the INTER-HEART study,⁸ with over 27,000 participants from 52 countries, BMI showed only a modest association with myocardial infarction between the top and bottom quintiles that was not significant after adjustment for other cardiovascular risk factors. In contrast, waist-to-hip ratio and waist circumference were strongly associated with myocardial infarction, even after adjustment for other risk factors. This study indicates that regional distribution of adiposity may be critical in determining the cardiovascular risk associated with obesity.

Other measures of fatness include skin fold thickness using calipers at specific body sites (i.e. trunk, thighs, shoulder blade, triceps, etc), bioelectric impedance, underwater weighing (densitometry), air displacement plethysmography, nuclear magnetic resonance (NMR), and hydrometry (dilution method).

As knowledge about fat depot heterogeneity increases, it has become clear that visualization of fat throughout the body may contribute additional important information towards the obesity phenotype and may be necessary in future clinical studies to advance the field.

Fat imaging modalities

Dual-Energy X-ray Absorptiometry (DXA)

DXA scanning uses low level x-rays that pass through different types of tissues at different rates providing estimates of fat mass, fat-free mass, and bone density. This method is widely used to measure bone density and can also accurately measure fat mass (table 1). A limitation of most DXA scanners is the capacity to image extremely obese persons. However, half body scans have been shown to provide an accurate body compositional analysis (figure 1).⁹ In this study, total fat mass, non-bone lean mass, or percent fat was comparable for the whole-body scans, left, and right side scans (>97% within individuals and >99.9% for the group). This study demonstrated that with new generation DXA, accurate, reproducible fat mass measurements can be obtained.

DXA is relatively simple to perform, less expensive and more accessible than magnetic resonance imaging or computed tomography. Radiation exposure is much less than computed tomography. Although subcutaneous and visceral fat cannot be clearly separated by DXA, abdominal fat mass determined by DXA correlates well with visceral fat as determined by other methods such as computed tomography and magnetic resonance imaging.¹⁰ The added prognostic information obtained by abdominal DXA scanning compared to simple waist circumference measurement is controversial.¹¹ In a study of postmenopausal women, DXA-derived abdominal fat mass and waist circumference were found to be of equal utility in predicting dyslipidemia.¹¹

Ultrasound

Ultrasound has been widely used as an effective technique to assess body fat composition for decades.¹² By using a portable imaging device, this technique is capable of making rapid estimates of fat in specific regions (figure 2).¹² Ultrasound is an attractive tool to evaluate obesity when other methods are not accessible (table 1). The major limitation of ultrasound is lack of standardization for measurements, so accuracy is dependent on operator proficiency.¹² Abdominal fat ultrasonography has been compared to anthropometric measurements of central obesity for prediction of the presence of coronary artery disease by computed tomography angiography.¹³ Patients with coronary artery disease had greater visceral fat thickness and a higher waist-to-hip ratio compared to those without coronary disease, while preperitoneal fat thickness, subcutaneous fat thickness and abdominal fat index were not correlated with coronary artery disease. However, after adjusting for traditional cardiovascular risk factors, only waist-to-hip ratio remained associated with coronary artery disease. Therefore, this study indicated that abdominal sonography measurement of fat indices was not superior to anthropometric measurements for prediction of coronary artery disease. Improvements in ultrasound devices and software designed specifically for the purpose of assessing fat composition may enhance the clinical utility of ultrasound.¹⁴

Transthoracic echocardiography (TTE), routinely used to analyze cardiac function, may be useful in measuring epicardial fat thickness overlying the right ventricle (figure 3).¹⁵ Human epicardial fat may be particularly relevant as it has been shown to be a source of local

inflammatory mediators,¹⁶ and could therefore promote atherosclerosis in the adjacent epicardial coronary arteries. Epicardial adipose tissue detected by TTE has shown a strong correlation with anthropometric and other imaging measurements of visceral adipose tissue. Therefore, TTE may represent a relatively easy and reliable imaging method for visceral adipose tissue prediction.^{17, 18} As with other ultrasound techniques, some studies have found poor reproducibility with echocardiogram measurements of epicardial fat thickness.¹⁹

Computed Tomography (CT)

X-ray computed tomography uses x-rays that are computer-processed to produce tomographic images of specific areas of a scanned object. From a large series of cross-sectional images taken around a single axis of rotation, a 3D image of the area of interest is created. This technology is now widely used for imaging in the medical field (table 1). Approximately 72 million scans were performed in the United States in 2007.²⁰

CT has been shown to be an excellent method for quantitating regional adiposity. CT has been used to provide ethnicity- and gender-specific visceral abdominal adipose tissue (VAT) and subcutaneous adipose tissue (SAT) prediction equations, derived from a large tri-ethnic sample. These equations will be useful in future studies of mechanisms of cardiometabolic disease across ethnicities in countries where imaging data are not available (figure 4).²¹

CT can also detect calcified and non-calcified atherosclerotic plaques in the vasculature, including the coronary arteries, so correlations can be made between volume of adipose tissue depots and vascular disease. As part of the Framingham Heart Study, 1155 participants without known cardiovascular disease underwent imaging with multidetector CT for quantification of VAT, intrathoracic fat, pericardial fat, and for quantification of aortic and coronary artery calcification.²² In this study, pericardial fat volume was defined as any adipose tissue located within the pericardium. Common cardiac risk factors, BMI, and waist circumference were also measured. Investigators found that both pericardial and intrathoracic fat correlated with waist circumference, BMI, VAT, hypertension, metabolic syndrome, diabetes, and dyslipidemia. These results strongly supported the adverse relationship between obesity, metabolic abnormalities and vascular disease. Of particular interest, however, was the finding that pericardial fat, but not intrathoracic fat, was associated with coronary artery calcification, even after adjustment for multiple variables and VAT. Similarly, intrathoracic, but not pericardial fat, was associated with calcification of the abdominal aorta. This intriguing finding suggested that fat depots surrounding vascular structures may exert local toxic effects that promote vascular disease, in addition to the adverse metabolic effects of generalized obesity. This study demonstrates the added information that could potentially be obtained with adipose tissue imaging by CT or other modalities. Epicardial fat is the adipose tissue accumulated between the visceral pericardium and the myocardium and may be particularly relevant given its direct contact with coronary arteries.²³ Preclinical studies have supported a complex role of brown, beige and white perivascular adipose tissue on a variety of vascular phenotypes.³ In addition to potential modulation of atherosclerosis, perivascular fat may contribute to formation of aortic aneurysms. Diseases of the aorta are not uncommon, contributing to approximately 16,000 deaths per year in the United States.²⁴ As part of the Framingham Heart Study, 3001 male

and female participants underwent imaging with CT for quantification of aortic dimensions and periaortic fat.²⁵ Investigators found that periaortic fat volumes were directly associated with thoracic and abdominal dimensions. This association was independent of other cardiac risk factors, including BMI and visceral adipose tissue volume. This study thus strongly supports a local effect of periaortic adipose tissue in aortic remodeling.

As CT imaging becomes increasingly practical and widespread, it must be kept in mind that the radiation doses are much higher than conventional x-ray. This can lead to significant radiation exposure, especially in subjects who receive repeated scans.²⁶ Ionizing radiation can cause DNA mutations linked to induction of cancer.²⁶ It is estimated that 1.5 – 2.0% of all cancers in the United States may be attributable to radiation from CT studies.²⁶

Magnetic Resonance Imaging (MRI)

Anatomic imaging of different fat depots can also be accomplished with MRI, and without the ionizing radiation required for CT (table 1). As with CT, MRI imaging protocols provide not only detailed images of fat depots but can also characterize disease processes in other organs that may be associated with different types of obesity. This is important since the association of obesity with vascular disease is complex with clear heterogeneity related to different types of adiposity. Imaging techniques that can simultaneously quantify vascular disease processes (or complications of disease processes) and accurately measure adipose depots may provide unique insight into associations between different patterns of adiposity and disease. For example, a recent study demonstrated that body fat distribution was a risk factor for cerebrovascular disease.²⁷ In a study of patients with MRI evidence of hyperacute ischemic stroke, MRI-based volumetric analysis of subcutaneous and visceral fat distribution was performed and then correlated with white matter lesion load (WMLL) by MRI and also total atherosclerotic plaque volume (TPV) by computed tomography angiography. These investigators found that neither total abdominal fat volume nor subcutaneous fat volume correlated with WMLL or TPV. However, when the specific volume of visceral adipose tissue was determined there was a direct correlation between a greater percentage of visceral adipose tissue and both WMLL and TPV.²⁷ Thus, even at sites distant from the disease process, this study suggests visceral adiposity is a risk factor for cerebrovascular disease.

MRI may also be useful for analyzing intrahepatic fat or hepatic steatosis that occurs in dysmetabolic syndromes. Hepatic steatosis may be risk factor/mediator for cardiovascular risk associated with obesity.²⁸ Liver biopsy is an invasive procedure and has sampling error. MRI can decompose the liver signal into fat and water components and measure liver fat more directly than ultrasound or CT.²⁹ Figure 5 shows an example of hepatic imaging in a subject with hepatic steatosis and severe dyslipidemia before and after treatment of the dyslipidemia with plasmapheresis and multidrug therapy.

Other organs may also be clinically useful to image for fat content. Skeletal muscle plays a key role in insulin resistance. Both intramyocellular and extramyocellular lipid content increase with obesity. Skeletal muscle triglyceride content, as determined by ¹H-nuclear magnetic resonance spectroscopy has been inversely correlated with insulin sensitivity in obese adolescents.³⁰ Myocardial fat may also be useful to image although differentiating

normal from pathologic fat infiltration by CT or MRI is often difficult.³¹ Pathologic conditions associated with myocardial fat include arrhythmogenic right ventricular dysplasia,³² healed myocardial infarction,³³ lipoma,³⁴ tuberous sclerosis,³⁵ and dilated cardiomyopathy.³⁶ In patients with lipodystrophy magnetic resonance spectroscopy has demonstrated cardiac steatosis associated with severe concentric left ventricular hypertrophy.³⁷ Fatty pancreas has also been recently described by MRI.³⁸ In one study, 16.1% of a community cohort met criteria for above normal levels of fat in the pancreas. Fatty pancreas was associated with central obesity, hypertriglyceridemia, and insulin resistance.³⁸

Positron Emission Tomography (PET)

While CT and MRI have been extremely informative in quantifying fat in depots and within organs, the analysis is largely limited to fat volumes. These techniques have reinforced the importance of anatomic, regional, fat heterogeneity, however, it remains unclear why certain regions of fat are more harmful than others. In vivo imaging techniques that can provide metabolic information specific to a particular fat storage site may add significantly to our understanding of adipose tissue in living humans (table 1).

PET detects gamma ray emissions from a molecule labeled with a positron-emitting tracer. Images are then constructed revealing a 3 dimensional representation of tracer activity at a particular site of interest. A widely used tracer is the glucose analog, 2-fluorodeoxy-D-glucose (2FDG). Concentrations of this tracer reflect tissue glucose uptake, serving as a surrogate for tissue metabolic activity. PET may be useful in phenotyping fat and has been used to track the heightened metabolic activity of brown adipose tissue (BAT) (figure 6).³⁹ The in vivo identification of BAT could be useful to monitor future therapies designed to promote transformation of white to more metabolically active brown fat. Recently, MRI has also been shown to reliably identify BAT that was confirmed histologically.⁴⁰

Regional differences in FDG activity have also been demonstrated among white adipose tissue depots. In a study of non-obese humans, adipose tissue volume was calculated with MRI and DXA, and dynamic PET FDG imaging was performed at baseline and following infusion of insulin.⁴¹ Visceral adipose tissue had higher rates of glucose uptake compared to subcutaneous adipose tissue, and glucose uptake correlated with systemic insulin sensitivity. Interestingly, VAT mass correlated negatively with glucose uptake and insulin sensitivity whereas no correlation was observed between subcutaneous fat mass and insulin sensitivity. These findings indicate regional differences exist between adipose depots related to insulin sensitivity and may shed light on the metabolically obese but normal-weight phenotype. FDG-PET imaging has also been performed in obese subjects.⁴² In this study, FDG uptake was higher in VAT compared to subcutaneous adipose tissue. Based on additional studies performed with stromal vascular cells from diet-induced obese mice,⁴² the authors speculated that the increased FDG uptake could be mediated by cells in the stromal vascular fraction of visceral adipose tissue.

PET and other nuclear imaging techniques may also be useful in the future to image blood flow and lymphatic transport in fat depots. The biological effect of an adipokine secreted from a fat depot may vary depending on whether it is transported via the lymphatic system

or capillaries. It has been demonstrated for example, that partitioning of adipokines to lymphatics or capillaries is a function of their molecular size.⁴³ Lymphatic drainage may also be impaired in adipose depots in obese subjects and this could affect local inflammatory response if there is impaired clearance of inflammatory cytokines such as tumor necrosis factor- α .⁴⁴

In Vivo Optical Imaging (Animals)

A simpler method to follow glucose utilization in smaller animal models utilized Cerendov luminescence imaging (CLI). CLI utilizes luminescence generated from the β^+ and β^- decay of radionuclides such as ^{18}F in the medium. It has been shown to identify brown adipose tissue activity in a mouse model (figure 7).⁴⁵ This method is cheaper and more feasible to employ than PET imaging and may be more practical for research laboratories (table 1).

Molecular imaging (Animals)

As interest in monitoring other molecules involved in adipose tissue phenotypes evolves, other imaging methods to track molecular activity of fat may be useful (table 1). In a recent study,⁴⁶ a novel peptide was identified that selectively binds to the vascular endothelium of brown adipose tissue, even in the absence of sympathetic nervous system stimulation. This peptide probe was used to identify brown adipose tissue depots in mice in conjunction with whole-body near-infrared fluorescence imaging (figure 8).⁴⁶

What can adipose tissue imaging tell us about patients and their diseases?

The utility of imaging adipose tissue will need to be studied in future clinical trials. Whether imaging will add additional prognostic information to relatively simple anthropometric measures, lipids, and serum biomarkers remains to be proven. One population that may benefit from additional adipose phenotyping is patients with type 2 diabetes. Although diabetes is considered a coronary disease equivalent, it has become clear that there is heterogeneity in the type 2 diabetic population with regards to cardiovascular risk, with apparent recent lowering of CV risk in the population as a whole.⁴⁷ However, the burden of comorbidities remains high and identification of high risk phenotypes will become increasingly important. There are many different drugs available to treat diabetes, some of which may be advantageous to a particular subgroup of diabetes with abundance of inflammatory visceral fat and high vascular risk. Those patients at high vascular risk may be treated differently than patients at low vascular risk. It may also be that specific therapies will be tailored to the particular organ involved. In one study of metabolic dysfunction, increased adiposity produced adverse metabolic effects that only correlated with the degree of intrahepatic triglyceride content.⁴⁸ Thus therapies targeting hepatic steatosis may be sufficient to treat metabolic derangements in certain patient subgroups. In addition to mediating metabolic derangements, hepatic steatosis may progress to steatohepatitis and fibrosis, which is a risk factor for cirrhosis and liver cancer.⁴⁹⁻⁵¹ Thus, noninvasive monitoring of hepatic steatosis may facilitate therapeutic interventions to prevent progression to more advanced liver disease. For example, the drug colesevelam was tested for reduction of liver fat, quantified by MRI, in patients with non-alcoholic steatohepatitis.⁵² A parallel study compared MRI-estimated proton density fat fraction (MRI-PDFF), which allows fat mapping of the entire liver to MR spectroscopy-PDFF, which provides a

biochemical measure of liver fat in small regions of interest.⁵³ Investigators found that MRI-PDFP correlated well with MRS-PDFP and was more sensitive than histology-determined steatosis grade in quantifying changes in liver fat content. Thus, hepatic MRI can be used to follow changes in liver fat. As knowledge of the pathophysiology of adipose tissue continues to grow, personalized, targeted therapeutic approaches may be most effective for preventing comorbidities and these approaches will be aided by adipose tissue imaging. These hypotheses will require validation in clinical trials.

Conclusion

Basic and preclinical studies have now clearly demonstrated marked heterogeneity between adipocytes and different fat depots. In parallel efforts, clinical and epidemiological studies have confirmed that different distributions of adiposity lead to different clinical outcomes. Thus, imaging of fat will likely become increasingly relevant for risk stratification and guiding future therapeutic interventions.

Acknowledgments

None.

Sources of Funding:

This work was supported by the National Institutes of Health (HL073150 to D.T.E.).

References

1. Rippe JM, Crossley S, Ringer R. Obesity as a chronic disease: Modern medical and lifestyle management. *J Am Diet Assoc.* 1998; 98:S9–15. [PubMed: 9787730]
2. Berall GB. Obesity: A crisis of growing proportions. *Paediatrics & child health.* 2002; 7:325–328. [PubMed: 20046313]
3. Brown NK, Zhou Z, Zhang J, Zeng R, Wu J, Eitzman DT, Chen YE, Chang L. Perivascular adipose tissue in vascular function and disease: A review of current research and animal models. *Arterioscler Thromb Vasc Biol.* 2014; 34:1621–1630. [PubMed: 24833795]
4. Omar A, Chatterjee TK, Tang Y, Hui DY, Weintraub NL. Proinflammatory phenotype of perivascular adipocytes. *Arterioscler Thromb Vasc Biol.* 2014; 34:1631–1636. [PubMed: 24925977]
5. Jarrett RJ. Is there an ideal body weight? *British medical journal.* 1986; 293:493–495. [PubMed: 3091177]
6. Eknayan G. Adolphe quetelet (1796-1874)--the average man and indices of obesity. *Nephrol Dial Transplant.* 2008; 23:47–51. [PubMed: 17890752]
7. Rothman KJ. Bmi-related errors in the measurement of obesity. *International journal of obesity.* 2008; 32(Suppl 3):S56–59. [PubMed: 18695655]
8. Yusuf S, Hawken S, Ounpuu S, et al. Obesity and the risk of myocardial infarction in 27,000 participants from 52 countries: A case-control study. *Lancet.* 2005; 366:1640–1649. [PubMed: 16271645]
9. Rothney MP, Brychta RJ, Schaefer EV, Chen KY, Skarulis MC. Body composition measured by dual-energy x-ray absorptiometry half-body scans in obese adults. *Obesity (Silver Spring).* 2009; 17:1281–1286. [PubMed: 19584885]
10. Park YW, Heymsfield SB, Gallagher D. Are dual-energy x-ray absorptiometry regional estimates associated with visceral adipose tissue mass? *Int J Obes Relat Metab Disord.* 2002; 26:978–983. [PubMed: 12080453]

11. Vatanparast H, Chilibeck PD, Cornish SM, Little JP, Paus-Jenssen LS, Case AM, Biem HJ. Dxa-derived abdominal fat mass, waist circumference, and blood lipids in postmenopausal women. *Obesity (Silver Spring)*. 2009; 17:1635–1640. [PubMed: 19343013]
12. Wagner DR. Ultrasound as a tool to assess body fat. *Journal of obesity*. 2013; 2013:280713. [PubMed: 24062944]
13. Shabestari AA, Bahrami-Motlagh H, Hosseinpanah F, Heidari K. Abdominal fat sonographic measurement compared to anthropometric indices for predicting the presence of coronary artery disease. *Journal of ultrasound in medicine : official journal of the American Institute of Ultrasound in Medicine*. 2013; 32:1957–1965. [PubMed: 24154900]
14. Utter AC, Hager ME. Evaluation of ultrasound in assessing body composition of high school wrestlers. *Medicine and science in sports and exercise*. 2008; 40:943–949. [PubMed: 18408602]
15. Chao TF, Hung CL, Tsao HM, et al. Epicardial adipose tissue thickness and ablation outcome of atrial fibrillation. *PLoS One*. 2013; 8:e74926. [PubMed: 24066158]
16. Mazurek T, Zhang L, Zalewski A, Mannion JD, Diehl JT, Arafat H, Sarov-Blat L, O'Brien S, Keiper EA, Johnson AG, Martin J, Goldstein BJ, Shi Y. Human epicardial adipose tissue is a source of inflammatory mediators. *Circulation*. 2003; 108:2460–2466. [PubMed: 14581396]
17. Iacobellis G, Assael F, Ribaldo MC, Zappaterreno A, Alessi G, Di Mario U, Leonetti F. Epicardial fat from echocardiography: A new method for visceral adipose tissue prediction. *Obes Res*. 2003; 11:304–310. [PubMed: 12582228]
18. Iacobellis G, Sharma AM. Epicardial adipose tissue as new cardio-metabolic risk marker and potential therapeutic target in the metabolic syndrome. *Curr Pharm Des*. 2007; 13:2180–2184. [PubMed: 17627550]
19. Saura D, Oliva MJ, Rodriguez D, Pascual-Figal DA, Hurtado JA, Pinar E, de la Morena G, Valdes M. Reproducibility of echocardiographic measurements of epicardial fat thickness. *Int J Cardiol*. 2010; 141:311–313. [PubMed: 19110328]
20. Berrington de Gonzalez A, Mahesh M, Kim KP, Bhargavan M, Lewis R, Mettler F, Land C. Projected cancer risks from computed tomographic scans performed in the united states in 2007. *Arch Intern Med*. 2009; 169:2071–2077. [PubMed: 20008689]
21. Eastwood SV, Tillin T, Wright A, Heasman J, Willis J, Godsland IF, Forouhi N, Whincup P, Hughes AD, Chaturvedi N. Estimation of ct-derived abdominal visceral and subcutaneous adipose tissue depots from anthropometry in europeans, south asians and african caribbeans. *PLoS One*. 2013; 8:e75085. [PubMed: 24069381]
22. Rosito GA, Massaro JM, Hoffmann U, Ruberg FL, Mahabadi AA, Vasan RS, O'Donnell CJ, Fox CS. Pericardial fat, visceral abdominal fat, cardiovascular disease risk factors, and vascular calcification in a community-based sample: The framingham heart study. *Circulation*. 2008; 117:605–613. [PubMed: 18212276]
23. Bertaso AG, Bertol D, Duncan BB, Foppa M. Epicardial fat: Definition, measurements and systematic review of main outcomes. *Arquivos brasileiros de cardiologia*. 2013; 101:e18–28. [PubMed: 23917514]
24. Isselbacher EM. Thoracic and abdominal aortic aneurysms. *Circulation*. 2005; 111:816–828. [PubMed: 15710776]
25. Thanassoulis G, Massaro JM, Corsini E, Rogers I, Schlett CL, Meigs JB, Hoffmann U, O'Donnell CJ, Fox CS. Periaortic adipose tissue and aortic dimensions in the framingham heart study. *Journal of the American Heart Association*. 2012; 1:e000885. [PubMed: 23316310]
26. Brenner DJ, Hall EJ. Computed tomography--an increasing source of radiation exposure. *N Engl J Med*. 2007; 357:2277–2284. [PubMed: 18046031]
27. Karcher HS, Holzwarth R, Mueller HP, Ludolph AC, Huber R, Kassubek J, Pinkhardt EH. Body fat distribution as a risk factor for cerebrovascular disease: An mri-based body fat quantification study. *Cerebrovascular diseases*. 2013; 35:341–348. [PubMed: 23615579]
28. Bhatia LS, Curzen NP, Calder PC, Byrne CD. Non-alcoholic fatty liver disease: A new and important cardiovascular risk factor? *Eur Heart J*. 2012; 33:1190–1200. [PubMed: 22408036]
29. Reeder SB, Cruite I, Hamilton G, Sirlin CB. Quantitative assessment of liver fat with magnetic resonance imaging and spectroscopy. *Journal of magnetic resonance imaging : JMRI*. 2011;34:spcone.

30. Sinha R, Dufour S, Petersen KF, LeBon V, Enoksson S, Ma YZ, Savoye M, Rothman DL, Shulman GI, Caprio S. Assessment of skeletal muscle triglyceride content by ¹H nuclear magnetic resonance spectroscopy in lean and obese adolescents: Relationships to insulin sensitivity, total body fat, and central adiposity. *Diabetes*. 2002; 51:1022–1027. [PubMed: 11916921]
31. Kimura F, Matsuo Y, Nakajima T, Nishikawa T, Kawamura S, Sannohe S, Hagiwara N, Sakai F. Myocardial fat at cardiac imaging: How can we differentiate pathologic from physiologic fatty infiltration? *Radiographics*. 2010; 30:1587–1602. [PubMed: 21071377]
32. Basso C, Thiene G. Adipositas cordis, fatty infiltration of the right ventricle, and arrhythmogenic right ventricular cardiomyopathy. Just a matter of fat? *Cardiovascular pathology : the official journal of the Society for Cardiovascular Pathology*. 2005; 14:37–41.
33. Goldfarb JW, Arnold S, Roth M, Han J. T1-weighted magnetic resonance imaging shows fatty deposition after myocardial infarction. *Magn Reson Med*. 2007; 57:828–834. [PubMed: 17457862]
34. Araoz PA, Mulvagh SL, Tazelaar HD, Julsrud PR, Breen JF. Ct and mr imaging of benign primary cardiac neoplasms with echocardiographic correlation. *Radiographics*. 2000; 20:1303–1319. [PubMed: 10992020]
35. Adriaensen ME, Schaefer-Prokop CM, Duyndam DA, Zonnenberg BA, Prokop M. Fatty foci in the myocardium in patients with tuberous sclerosis complex: Common finding at ct. *Radiology*. 2009; 253:359–363. [PubMed: 19709996]
36. Kaminaga T, Naito H, Takamiya M, Hamada S, Nishimura T. Myocardial damage in patients with dilated cardiomyopathy: Ct evaluation. *Journal of computer assisted tomography*. 1994; 18:393–397. [PubMed: 8188904]
37. Nelson MD, Victor RG, Szczepaniak EW, Simha V, Garg A, Szczepaniak LS. Cardiac steatosis and left ventricular hypertrophy in patients with generalized lipodystrophy as determined by magnetic resonance spectroscopy and imaging. *Am J Cardiol*. 2013; 112:1019–1024. [PubMed: 23800548]
38. Wong VW, Wong GL, Yeung DK, Abrigo JM, Kong AP, Chan RS, Chim AM, Shen J, Ho CS, Woo J, Chu WC, Chan HL. Fatty pancreas, insulin resistance, and beta-cell function: A population study using fat-water magnetic resonance imaging. *Am J Gastroenterol*. 2014; 109:589–597. [PubMed: 24492753]
39. Muzik O, Mangner TJ, Granneman JG. Assessment of oxidative metabolism in brown fat using pet imaging. *Frontiers in endocrinology*. 2012; 3:15. [PubMed: 22649408]
40. Reddy NL, Jones TA, Wayte SC, Adesanya O, Sankar S, Yeo YC, Tripathi G, McTernan PG, Randeve HS, Kumar S, Hutchinson CE, Barber TM. Identification of brown adipose tissue using mr imaging in a human adult with histological and immunohistochemical confirmation. *J Clin Endocrinol Metab*. 2014; 99:E117–121. [PubMed: 24384025]
41. Ng JM, Azuma K, Kelley C, Pencek R, Radikova Z, Laymon C, Price J, Goodpaster BH, Kelley DE. Pet imaging reveals distinctive roles for different regional adipose tissue depots in systemic glucose metabolism in nonobese humans. *Am J Physiol Endocrinol Metab*. 2012; 303:E1134–1141. [PubMed: 22967498]
42. Christen T, Sheikine Y, Rocha VZ, Hurwitz S, Goldfine AB, Di Carli M, Libby P. Increased glucose uptake in visceral versus subcutaneous adipose tissue revealed by pet imaging. *JACC Cardiovasc Imaging*. 2010; 3:843–851. [PubMed: 20705265]
43. Miller NE, Michel CC, Nanjee MN, Olszewski WL, Miller IP, Hazell M, Olivecrona G, Sutton P, Humphreys SM, Frayn KN. Secretion of adipokines by human adipose tissue in vivo: Partitioning between capillary and lymphatic transport. *Am J Physiol Endocrinol Metab*. 2011; 301:E659–667. [PubMed: 21750269]
44. Arngrim N, Simonsen L, Holst JJ, Bulow J. Reduced adipose tissue lymphatic drainage of macromolecules in obese subjects: A possible link between obesity and local tissue inflammation? *International journal of obesity*. 2013; 37:748–750. [PubMed: 22751255]
45. Zhang X, Kuo C, Moore A, Ran C. In vivo optical imaging of interscapular brown adipose tissue with ¹⁸F-fdg via cerenkov luminescence imaging. *PLoS One*. 2013; 8:e62007. [PubMed: 23637947]

46. Azhdarinia A, Daquinag AC, Tseng C, Ghosh SC, Ghosh P, Amaya-Manzanares F, Sevic-Muraca E, Kolonin MG. A peptide probe for targeted brown adipose tissue imaging. *Nature communications*. 2013; 4:2472.
47. Gregg EW, Li Y, Wang J, Burrows NR, Ali MK, Rolka D, Williams DE, Geiss L. Changes in diabetes-related complications in the united states, 1990-2010. *N Engl J Med*. 2014; 370:1514–1523. [PubMed: 24738668]
48. Magkos F, Fabbrini E, Mohammed BS, Patterson BW, Klein S. Increased whole-body adiposity without a concomitant increase in liver fat is not associated with augmented metabolic dysfunction. *Obesity (Silver Spring)*. 2010; 18:1510–1515. [PubMed: 20395947]
49. Adams LA, Sanderson S, Lindor KD, Angulo P. The histological course of nonalcoholic fatty liver disease: A longitudinal study of 103 patients with sequential liver biopsies. *J Hepatol*. 2005; 42:132–138. [PubMed: 15629518]
50. Ekstedt M, Franzen LE, Mathiesen UL, Thorelius L, Holmqvist M, Bodemar G, Kechagias S. Long-term follow-up of patients with naflid and elevated liver enzymes. *Hepatology*. 2006; 44:865–873. [PubMed: 17006923]
51. Ascha MS, Hanouneh IA, Lopez R, Tamimi TA, Feldstein AF, Zein NN. The incidence and risk factors of hepatocellular carcinoma in patients with nonalcoholic steatohepatitis. *Hepatology*. 2010; 51:1972–1978. [PubMed: 20209604]
52. Le TA, Chen J, Changchien C, Peterson MR, Kono Y, Patton H, Cohen BL, Brenner D, Sirlin C, Loomba R, San Diego Integrated NRC. Effect of colesvelam on liver fat quantified by magnetic resonance in nonalcoholic steatohepatitis: A randomized controlled trial. *Hepatology*. 2012; 56:922–932. [PubMed: 22431131]
53. Nouredin M, Lam J, Peterson MR, Middleton M, Hamilton G, Le TA, Bettencourt R, Changchien C, Brenner DA, Sirlin C, Loomba R. Utility of magnetic resonance imaging versus histology for quantifying changes in liver fat in nonalcoholic fatty liver disease trials. *Hepatology*. 2013; 58:1930–1940. [PubMed: 23696515]
54. Chen W, Wilson JL, Khaksari M, Cowley MA, Enriori PJ. Abdominal fat analyzed by dexta scan reflects visceral body fat and improves the phenotype description and the assessment of metabolic risk in mice. *Am J Physiol Endocrinol Metab*. 2012; 303:E635–643. [PubMed: 22761161]
55. Borkan GA, Gerzof SG, Robbins AH, Hults DE, Silbert CK, Silbert JE. Assessment of abdominal fat content by computed tomography. *Am J Clin Nutr*. 1982; 36:172–177. [PubMed: 7091027]
56. Staten MA, Totty WG, Kohrt WM. Measurement of fat distribution by magnetic resonance imaging. *Investigative radiology*. 1989; 24:345–349. [PubMed: 2745015]
57. van Marken Lichtenbelt WD, Vanhommerig JW, Smulders NM, Drossaerts JM, Kemerink GJ, Bouvy ND, Schrauwen P, Teule GJ. Cold-activated brown adipose tissue in healthy men. *N Engl J Med*. 2009; 360:1500–1508. [PubMed: 19357405]

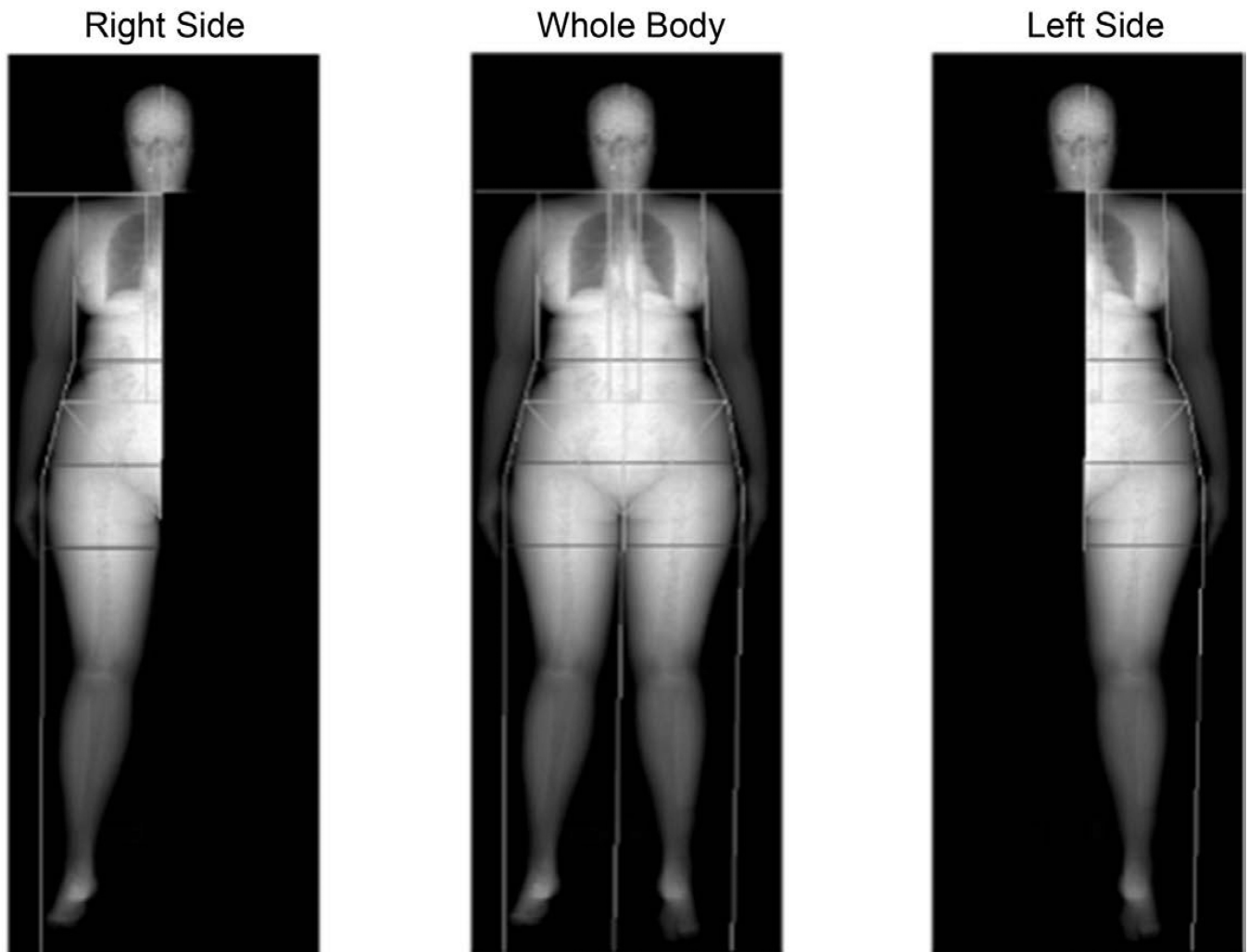


Figure 1. Body composition measured by dual-energy X-ray absorptiometry half-body scans in obese children. Example of iDXA total-body composition image and a representation of the portions of the total-body image used to generate the right side and left side images. (Reproduced from ref 9)

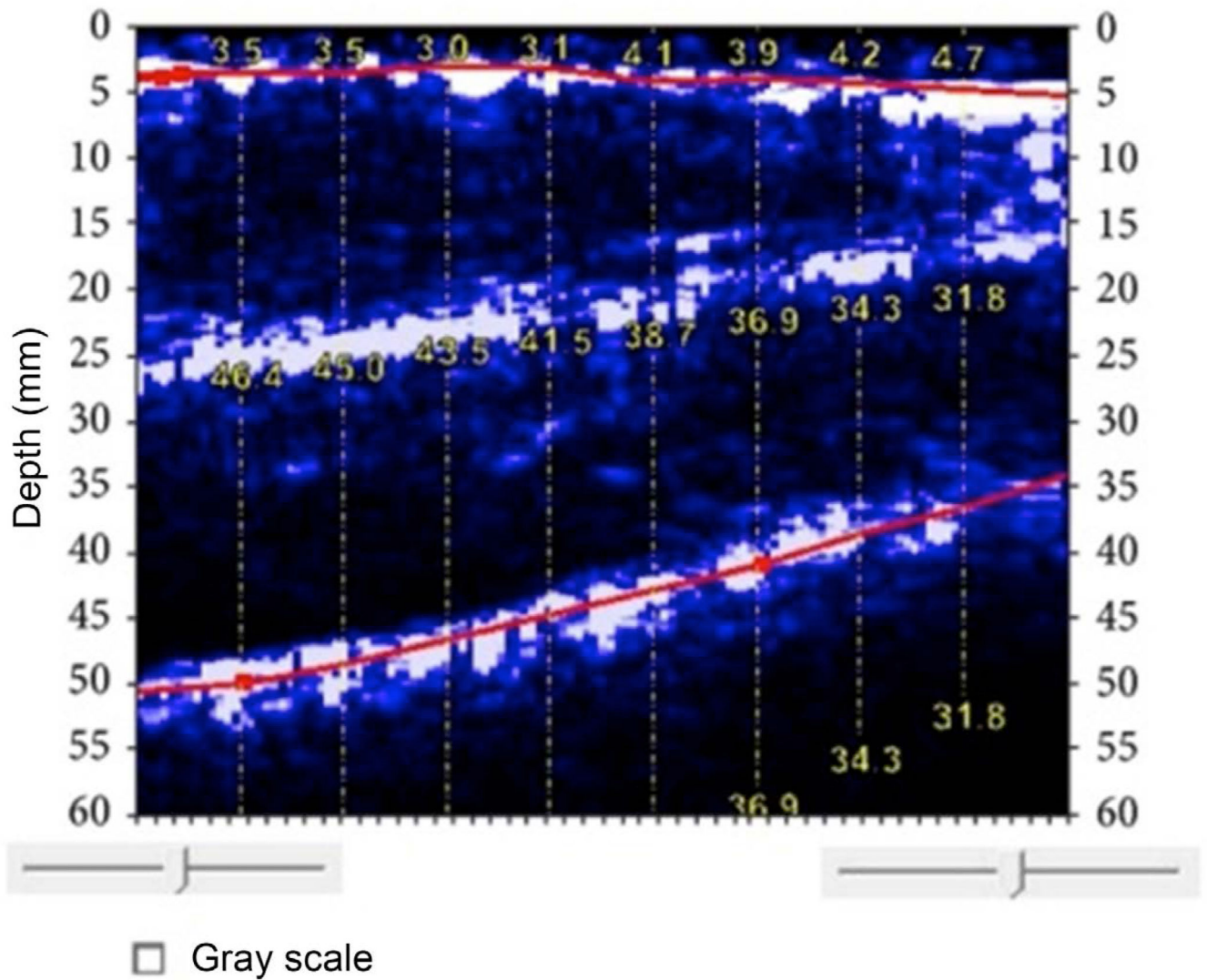


Figure 2. BodyMetric ultrasound image of thigh. The top line indicates the subcutaneous fat-muscle interface (average thickness of 3.69 mm). The bottom line indicates the muscle-bone boundary. The muscle thickness ranges from 32.0 mm to 46.6 mm. The white layer in the center is the boundary of the rectus femoris and vastus intermedius. (Reproduced from ref 12)

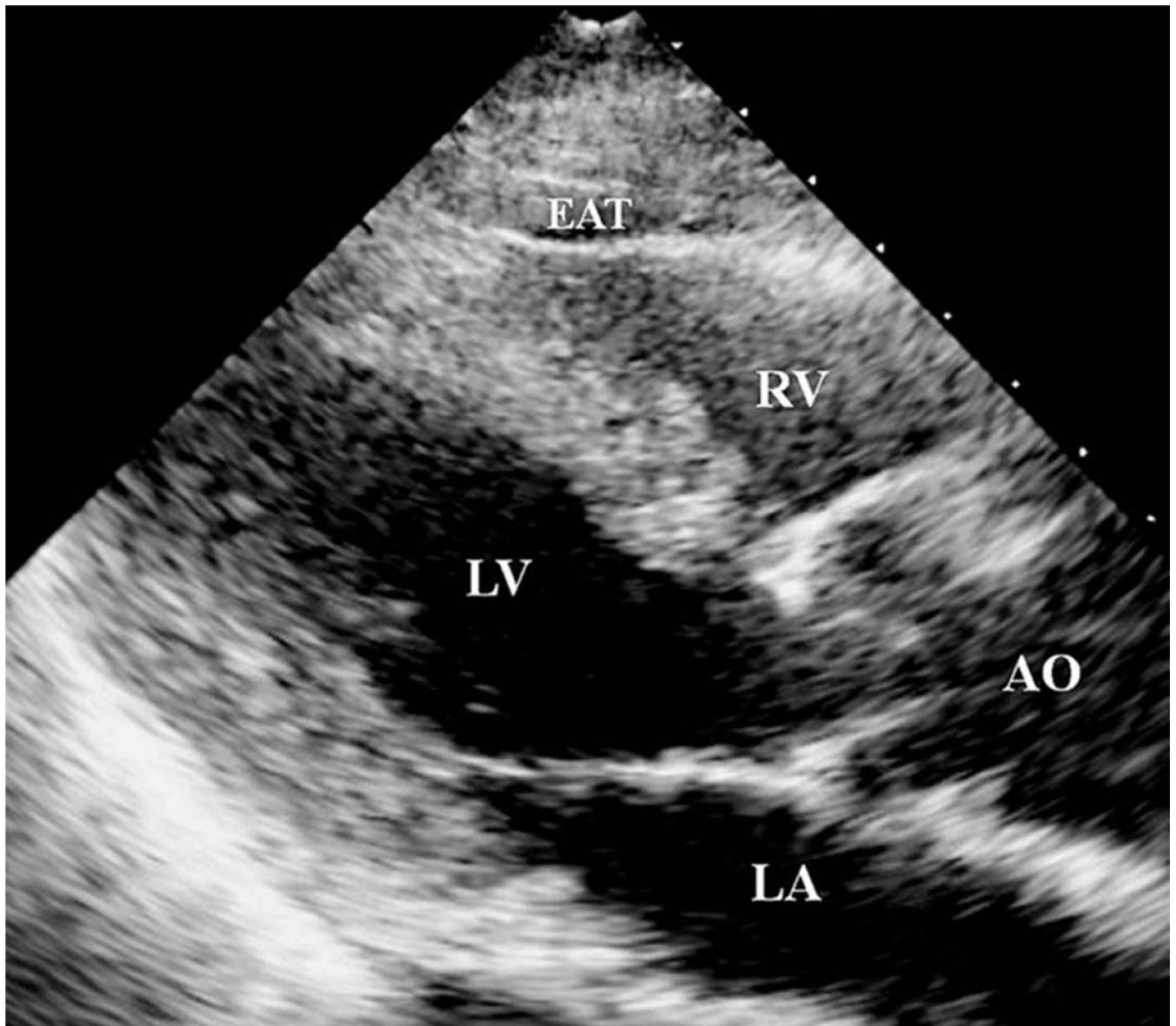


Figure 3. Measurement of epicardial adipose tissue measured in parasternal long-axis view of TTE. AO = aorta; EAT = epicardial adipose tissue; LA = left atrium; LV = left ventricle; RV = right ventricle. (Reproduced from ref 15)



Figure 4. Measurement of visceral adipose tissue and subcutaneous adipose tissue from CT image at L4. Adipose tissue is dark grey, white line shows delineation of visceral compartment, white arrow indicates depth of subcutaneous compartment. (Reproduced from ref 21)

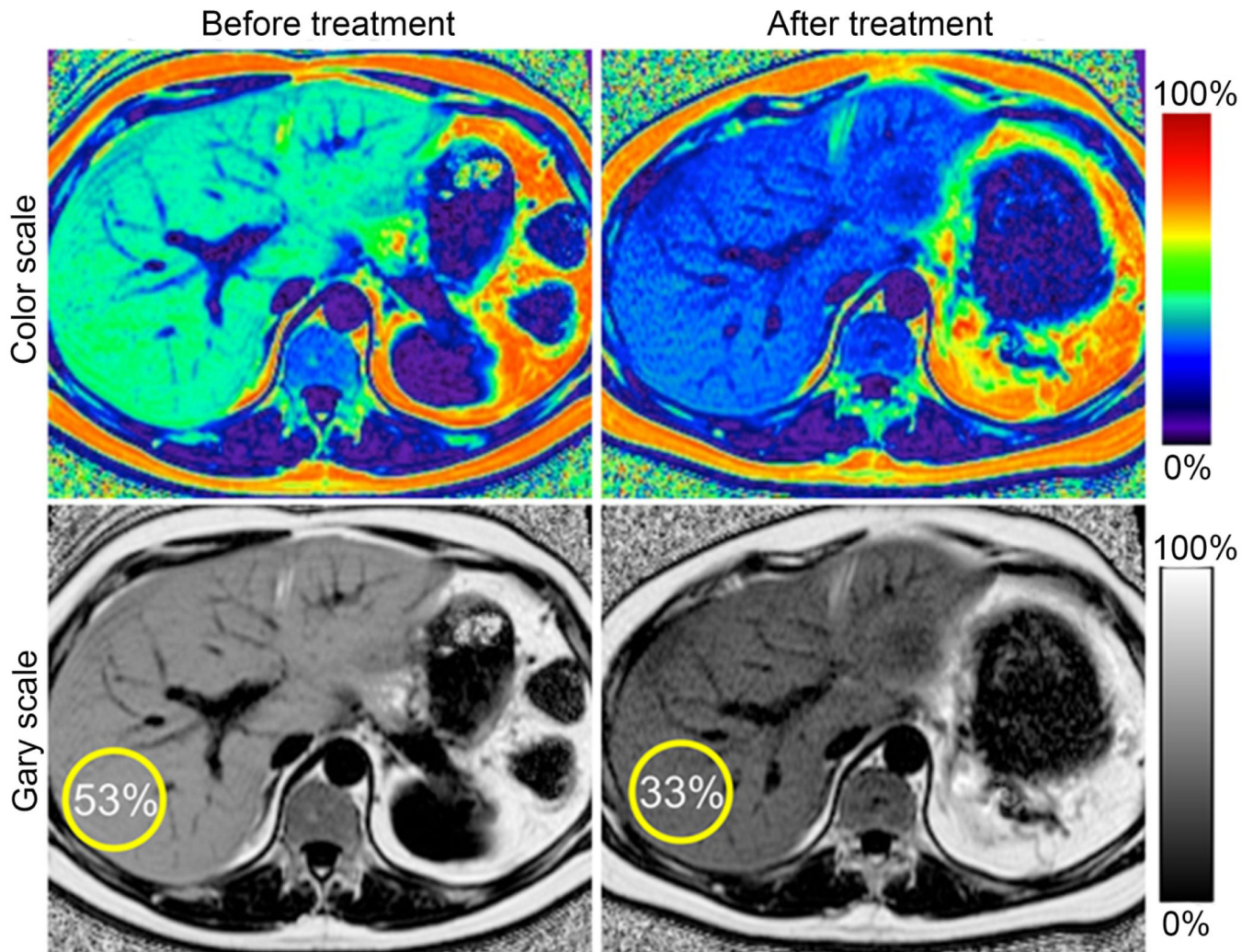


Figure 5.

Serial liver MRI scans to demonstrate changes in liver fat during therapy. Serial proton density fat-fraction (PDFF) maps obtained with complex-based MRI were acquired in a 41 year-old man with hypertriglyceridemia and insulin resistance undergoing plasmapheresis and multi-drug therapy to lower serum triglycerides. Follow-up MRI demonstrates reduction in hepatic PDFF (from 53% to 33%). (Reproduced from ref 29)

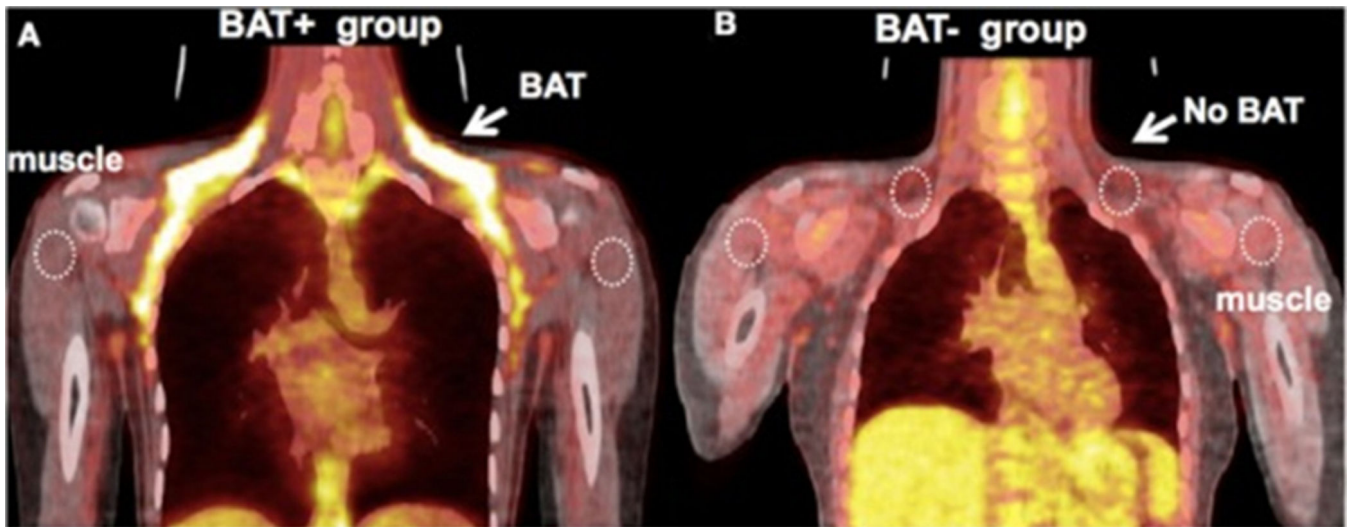


Figure 6.

A. Representative image of a subject with high uptake of FDG in BAT. B. Representative image of a subject from the BAT- group – there is an absence of FDG uptake at the location of BAT following exposure to cold. (Reproduced from ref 39)

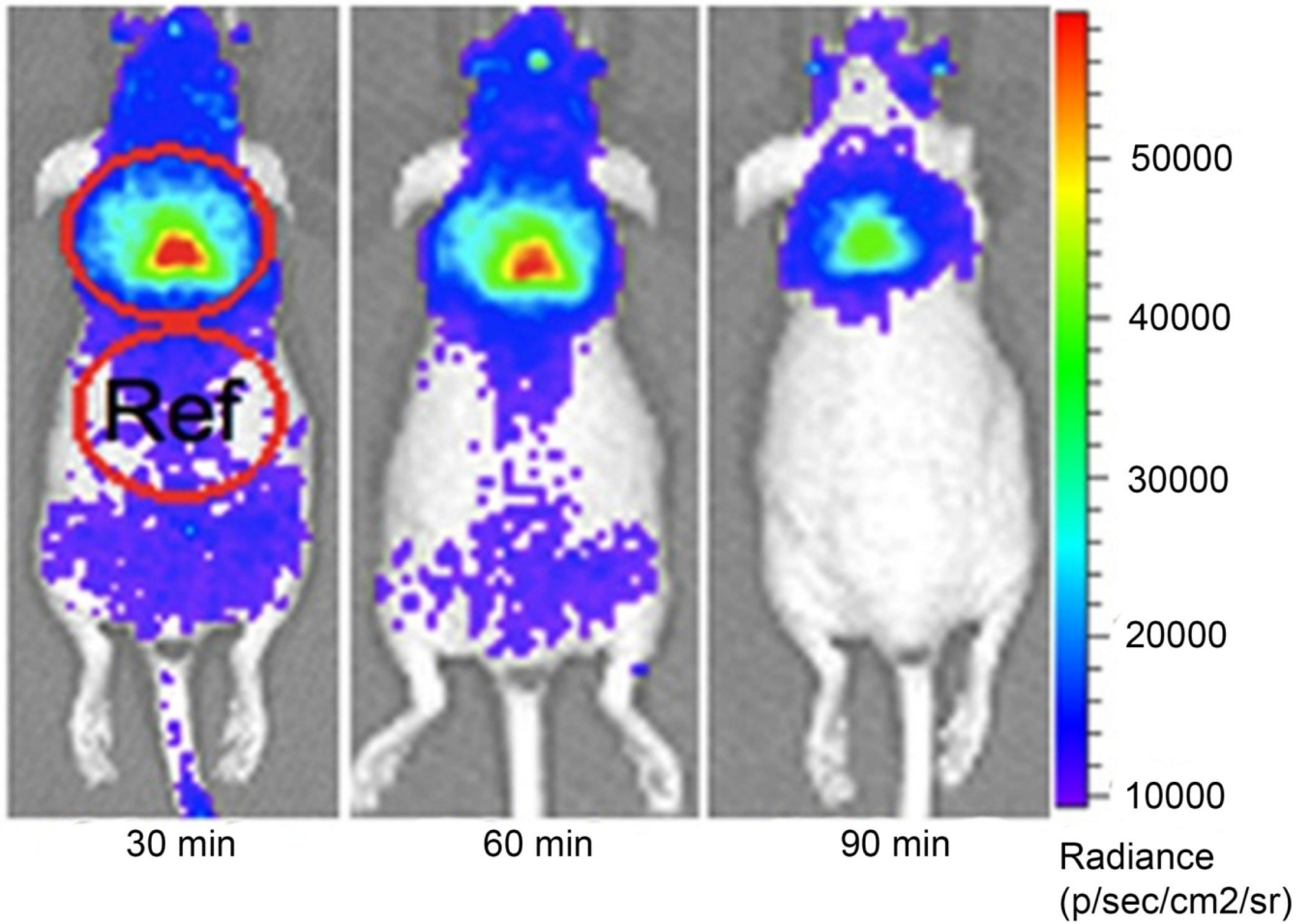


Figure 7. CLI images of interscapular BAT in a mouse at 30, 60, 120 minutes after ^{18}F -FDG (10.3 MBq) intravenous injection. The images clearly outline the contour of BAT, even after 120 minutes of ^{18}F -FDG injection. (Reproduced from ref 45)

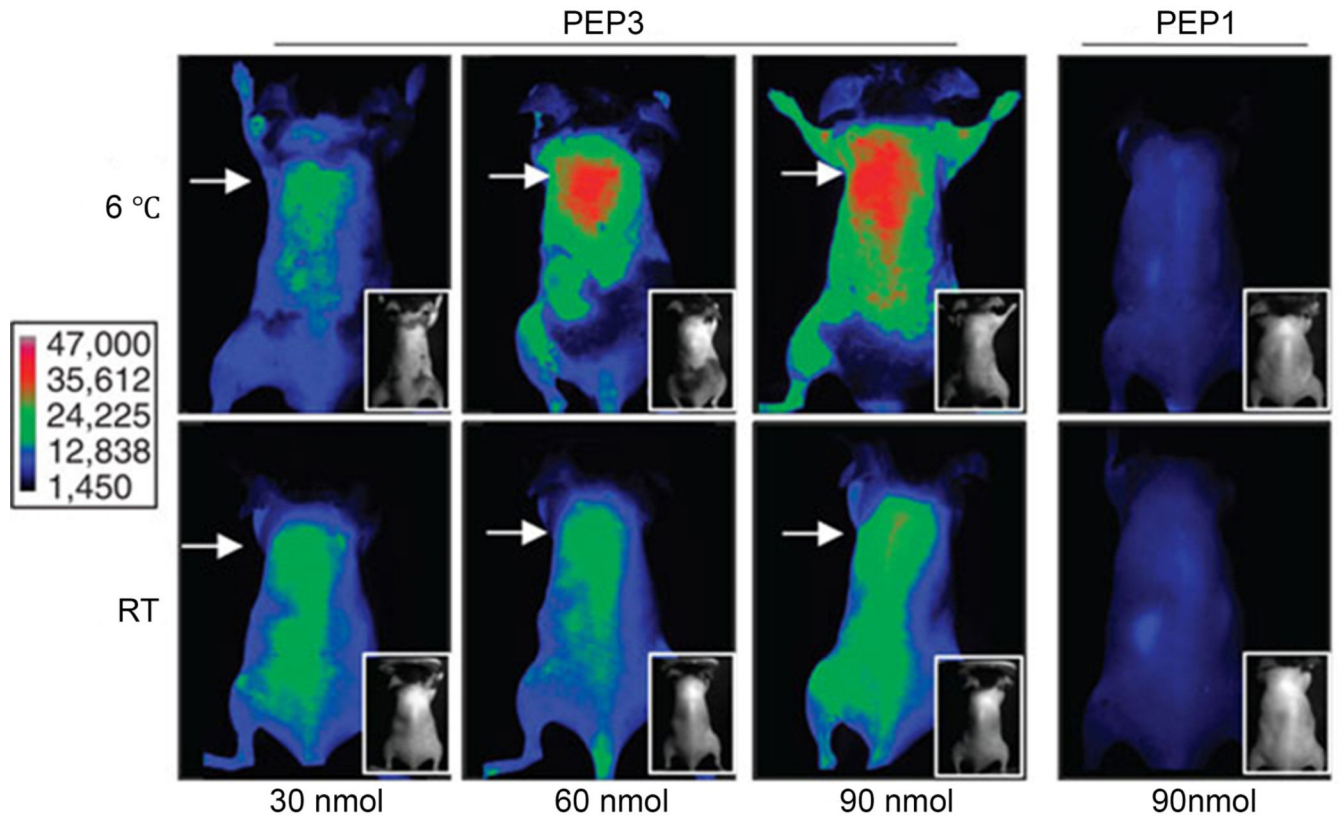


Figure 8.

Whole-body near-infrared-fluorescence imaging of cold (6°C) or warm (RT) -acclimated mice 1h after i.v. administration of indicated doses of IRDye800-conjugated phage clones displaying peptide (PEP), PEP3 (which recognizes brown fat vasculature) or control peptide PEP1. Arrow indicates interscapular area. Insets show black/white photographs of mice that were shaved for imaging (skin left on). Scale shows fluorescence intensity. (Reproduced from ref 46)

Table 1

Comparison of different adipose tissue imaging techniques.

Measure	Techniques	Advantages	Disadvantages	References
Fat mass	DXA	low radiation, short imaging time	Expensive, hard to distinguish between subcutaneous fat and visceral fat	Chen W, et al. ⁵⁴
Fat mass	Ultrasound	Lower cost, easy, no radiation	Low accuracy	Wagner DR. ¹²
Fat mass	CT	Accurate, measures specific body fat compartments	Expensive, higher radiation	Borkan, GA, et al. ⁵⁵
Fat mass	MRI	Accurate, measures specific body fat compartments, no radiation	Expensive	Staten MA, et al. ⁵⁶
Fat metabolism	PET	Accurate, measures body fat compartments and metabolism including brown fat	Expensive, radiation	van Marken Linchtenbelt WD, et al. ⁵⁷
Fat metabolism	In vivo optical imaging	Accurate, lower cost	Radiation, not widely used in humans	Zhag X, et al. ⁴⁵
Fat metabolism	Molecular imaging	Accurate, lower cost	Only used in animals	Azhdarinia A, et al. ⁴⁶